



Published in final edited form as:

J Nat Prod. 2017 July 28; 80(7): 1981–1991. doi:10.1021/acs.jnatprod.6b01129.

Withanolides from Aeropically Grown *Physalis peruviana* and Their Selective Cytotoxicity to Prostate Cancer and Renal Carcinoma Cells

Ya-Ming Xu[†], E. M. Kithsiri Wijeratne[†], Ashley L. Babyak[‡], Hanna R. Marks[‡], Alan D. Brooks[‡], Poonam Tewary[‡], Li-Jiang Xuan[§], Wen-Qiong Wang[§], Thomas J. Sayers[‡], A. A. Leslie Gunatilaka^{*,†}

[†]Natural Products Center, School of Natural Resources and the Environment, College of Agriculture and Life Sciences, University of Arizona, 250 E. Valencia Road, Tucson, Arizona 85706, United States

[‡]Basic Research Program, Leidos Biomedical Research, Inc., Frederick National Laboratory for Cancer Research, and Cancer and Inflammation Program, National Cancer Institute, Frederick, Maryland 21702, United States

[§]State Key Laboratory of Drug Research, Shanghai Institute of Materia Medica, Chinese Academy of Sciences, 501 Haike Road, Zhangjiang Hi-Tech Park, Shanghai 201203, People's Republic of China

Abstract

Investigation of aeropically grown *Physalis peruviana* resulted in the isolation of 11 new withanolides, including perulactones I–L (**1–4**), 17-deoxy-23 β -hydroxywithanolide E (**5**), 23 β -hydroxywithanolide E (**6**), 4-deoxyhyperunolide A (**7**), 7 β -hydroxywithanolide F (**8**), 7 β -hydroxy-17-*epi*-withanolide K (**9**), 24,25-dihydro-23 β ,28-dihydroxywithanolide G (**10**), and 24,25-dihydroxywithanolide E (**11**), together with 14 known withanolides (**12–25**). The structures of **1–11** were elucidated by the analysis of their spectroscopic data, and **12–25** were identified by comparison of their spectroscopic data with those reported. All withanolides were evaluated for their cytotoxic activity against a panel of tumor cell lines including LNCaP (androgen-sensitive human prostate adenocarcinoma), 22Rv1 (androgen-resistant human prostate adenocarcinoma), ACHN (human renal adenocarcinoma), M14 (human melanoma), SK-MEL-28 (human melanoma), and normal human foreskin fibroblast cells. Of these, the 17 β -hydroxywithanolides (17-BHWs) **6**, **8**, **9**, **11–13**, **15**, and **19–22** showed selective cytotoxic activity against the two prostate cancer cell lines LNCaP and 22Rv1, whereas **13** and **20** exhibited selective toxicity for the ACHN renal carcinoma cell line. These cytotoxicity data provide additional structure–activity relationship information for the 17-BHWs.

*Corresponding Author: Tel (A. A. L. Gunatilaka): (520) 621-9932. Fax: (520) 621-8378. leslieg1@email.arizona.edu.

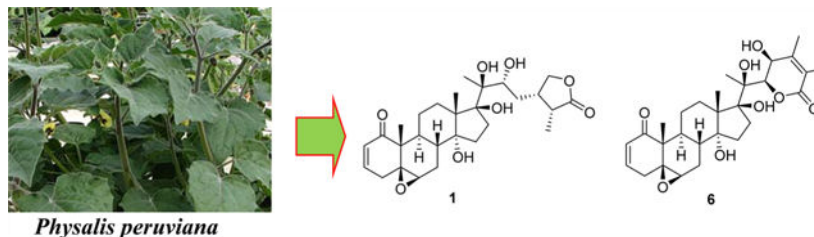
Supporting Information

The Supporting Information is available free of charge on the ACS Publications website at DOI: 10.1021/acs.jnat-prod.6b01129.

¹H, ¹³C, and 2D NMR spectra of withanolides **1–11**, key HMBC and COSY correlations for **1**, **3**, **5**, and **7–11**, key NOESY correlations for **1**, **3–5**, and **7–11**, and ECD spectra for **1–11** (PDF)

The authors declare no competing financial interest.

Graphical Abstract



Prostate cancer (PC), a hormone-sensitive cancer that is influenced by androgens such as testosterone,¹ is one of the most frequent solid tumors in older men and the second leading cancer killer of all men in North America.² Androgen deprivation is still the standard therapy used to treat the metastatic disease,³ but patients invariably relapse with more aggressive androgen-insensitive PC. Despite the success of recently approved PC therapies targeting androgen receptor (AR) signaling (e.g., abiraterone)⁴ and second-generation antiandrogens (e.g., enzalutamide),⁵ durable responses appear to be limited, presumably due to acquired resistance. Moreover, androgen-insensitive PC resumes expression of multiple AR-regulated genes, such as prostate-specific antigen (PSA), suggesting that AR transcriptional activity becomes reactivated at this stage of the disease.⁶ Therefore, targeting both androgen-sensitive and androgen-insensitive cancer cells is important in PC drug discovery efforts. Renal carcinoma (RC) is among the 10 most common cancers in the U.S.⁷ Current therapies for RC include antiangiogenic and immunotherapies, which have shown only modest success for patients with advanced RC.⁸ Thus, the search for effective drugs to treat advanced PC and RC is considered a priority in anticancer drug discovery.

Physalis peruviana L. (family: Solanaceae) is a member of a genus with about 120 species,⁹ of which some are employed in traditional medicine in Asia and South America.¹⁰ Over 160 steroidal lactones belonging to the withanolide group have been reported from plants of this genus, and the ethnopharmacological activities of many *Physalis* species used in traditional medicines have been attributed to the presence of these withanolides.^{9,10} Previous phytochemical investigations of *P. peruviana* have resulted in the isolation of over 40 withanolides.¹¹ Of these, 4 β -hydroxywithanolide E (**12**), withanolide E (**13**), phyperunolide A (**14**), and withanolide C (**27**) have been reported to be cytotoxic to cell lines derived from lung cancer (A549),^{11f} liver carcinomas (Hep G2 and Hep 3B),^{11f} and breast adenocarcinomas (MCF-7 and MDA-MB-231).^{11f} In addition, **12** was found to inhibit proliferation of MCF-7,^{11j} MDA-MB-231,^{11j} H1299 (lung cancer),^{11h} Ca9-22 (oral cancer),^{11k} and HT-29 (colorectal cancer)¹¹ⁿ cells. We have recently reported that withanolide E (**13**), isolated from wild-crafted *P. peruviana*, was able to eliminate long-term survival of RC cells (ACHN, Caki-1, and SN-12-C) in the presence of TRAIL (tumor necrosis factor-related apoptosis-inducing ligand).¹² In our continuing search for natural-product-based anticancer agents,¹³ we have investigated aeroponically grown *P. peruviana*, and herein we report the isolation of 25 withanolides, of which some exhibited selective cytotoxicity for the androgen-sensitive PC (LNCaP), androgen-insensitive PC (22Rv1), and RC (ACHN) cell lines. Eleven of the withanolides encountered are new, and these were identified as perulactones I-L (**1–4**), 17-deoxy-23 β -hydroxywithanolide E (**5**), 23 β -hydroxywithanolide

E (**6**), 4-deoxyphyperunolide A (**7**), 7 β -hydroxywithanolide F (**8**), 7 β -hydroxy-17-*epi*-withanolide K (**9**), 24,25-dihydro-23 β ,28-dihydroxywithanolide G (**10**), and 24,25-dihydrowithanolide E (**11**). Comparison of spectroscopic data with those reported led to the identification of previously known withanolides as 4 β -hydroxywithanolide E (**12**),¹⁴ withanolide E (**13**),¹⁴ phyperunolide A (**14**),^{11f} withangulatin E (**15**),¹⁵ withanolide S 5-methyl ether (**16**),¹⁶ physalolactone (**17**),¹⁷ withanolide S (**18**),¹⁸ withaperuvin L (**19**),¹¹ⁱ physapruin A (**20**),¹⁹ withaperuvin J (**21**),¹¹ⁱ withanolide F (**22**),²⁰ 4-deoxyphysalolactone (**23**),¹⁷ perulactone B (**24**),¹⁴ and perulactone H (**25**).¹⁴

RESULTS AND DISCUSSION

Withanolides **1–4** were obtained as colorless, amorphous solids. Their ¹H NMR and ¹³C NMR data (Tables 1 and 3) indicated the presence of a γ -lactone side chain similar to those of perulactone and perulactone B (**24**),^{11i,14} and therefore **1–4** were designated as perulactones I–L. The molecular formula of perulactone I (**1**) was determined to be C₂₈H₄₀O₈ based on its HRESIMS and NMR data, suggesting nine degrees of unsaturation. Comparison of its molecular formula and NMR data with those of perulactone B (**24**) (C₂₈H₄₀O₇) also encountered in this study suggested that the ring B 5,6-ene moiety in **24** was probably replaced by a 5 β ,6 β -epoxide moiety [δ_{H} 3.19 (1H, d, J = 2.0 Hz, H-6); δ_{C} 62.1 (C-5) and 64.0 (C-6)] in **1**. In addition, its HMBC data (Figures S4 and S59, Supporting Information) showed the presence of long-range correlations of H-19 (δ_{H} 1.26)/C-1 (δ_{C} 203.8), H-3 (δ_{H} 6.85)/C-1, H-19/C-5 (δ_{C} 62.1), H-4 β (δ_{H} 2.96)/C-6 (δ_{C} 64.0), H-18 (δ_{H} 1.08)/C-14 (δ_{C} 83.2), H-18/C-17 (δ_{C} 88.3), H-21 (δ_{H} 1.22)/C-17, H-21/C-22 (δ_{C} 72.3), H-27 (δ_{H} 1.16)/C-26 (δ_{C} 180.8), and H-28 (δ_{H} 4.39 and 4.06)/C-25 (δ_{C} 37.7), further supporting the presence of a 5,6-epoxide moiety and a perulactone-type side chain in **1**. The β -orientation of the 5,6-epoxide was confirmed by a NOESY correlation between H-6 (δ_{H} 3.19) and H-4 α (δ_{H} 1.92) (Figures S5 and S60, Supporting Information). The *cis*-linkage of A and B rings in **1** was established by the strong positive Cotton effect at 340 nm in its electronic circular dichroism (ECD) spectrum²¹ (Figure S61, Supporting Information). Epoxidation of perulactone B (**24**) with *m*-CPBA²² afforded a major product that was identical with **1**. Perulactone I was thus identified as (24*S*,25*R*)-5 β ,6 β -epoxy-14 α ,17 β ,20 β ,22 α ,28-pentahydroxy-1-oxo-ergosta-2-en-26-oic acid γ -lactone (**1**).

Perulactone J (**2**) was determined to have the molecular formula C₂₈H₄₀O₆, corresponding to nine degrees of unsaturation. The ¹H NMR spectrum of **2** contained three olefinic protons [δ_{H} 6.77 (1H, ddd, J = 10.0, 4.8, 2.4 Hz, H-3), 5.87 (1H, dd, J = 10.0, 2.0 Hz, H-2), 5.59 (1H, brd, J = 5.6 Hz, H-6)], indicating the presence of ring A 2,3-en-1-one and ring B 5,6-ene moieties as in perulactone B (**24**).¹⁴ Comparison of the ¹³C NMR data of **2** and **24** revealed that the typical tetrasubstituted oxygenated carbon (C-17) signal at δ_{C} 87.0 in **24**¹⁴ was replaced by a methine signal at δ_{C} 49.4 in **2**. The long-range correlations observed for H₃-18 (δ_{H} 1.03)/C-17 (δ_{C} 49.7) and H₃-21 (δ_{H} 1.20)/C-17 in the HMBC spectrum of **2** (Figure 2) confirmed the presence of the CH-17 moiety. The NOE correlation between CH₃-18 and CH₃-21 in the 1D NOESY spectrum (Figure 2) suggested that the orientation of the side chain is β . Thus, the orientation of H-17 should be α . The ECD spectrum of **2** showed a negative Cotton effect at 339 nm, which is the opposite of that observed for **1**. This

difference may be due to the conformational changes of rings A and B of these two compounds caused by the replacement of the 5 β ,6 β -epoxide with a 5,6-ene moiety. The structure of perulactone J was thus elucidated as (17*S*,24*S*,25*R*)-14 α ,20 β ,22 α ,28-tetrahydroxy-1-oxo-ergosta-2,5-dien-26-oic acid γ -lactone (**2**).

The molecular formula of perulactone K (**3**) (C₂₈H₃₈O₆) and its ¹H and ¹³C NMR data (Tables 1 and 3) suggested that it is a dehydrated analogue of perulactone I (**1**) (C₂₈H₄₀O₈) lacking an oxygen atom. Comparison of its ¹H NMR data with those of **1** suggested that **3** contains a signal due to an olefinic proton [δ_{H} 5.71 (1H, dd, J = 2.4, 1.2 Hz, H-16)] besides signals due to four methyl groups, 2,3-en-1-one, 5 β ,6 β -epoxide, and the side chain γ -lactone moieties. The ¹³C NMR data (Table 3) of **3** also contained signals typical of other perulactones, including 2,3-en-1-one [δ_{C} 203.3 (C-1), 144.3 (C-3), 129.3 (C-2)], 5 β ,6 β -epoxide [δ_{C} 63.2 (C-6), 62.1 (C-5)], and the side chain γ -lactone [δ_{C} 180.3 (C-26), 72.4 (C-28)]. The ¹³C NMR spectrum **3** indicated the presence only two oxygenated carbons [δ_{C} 76.7 (C-20), 74.6 (C-22)]. The HMBC correlations observed for H₃-18 (δ_{H} 0.94)/C-14 (δ_{C} 58.1), H₃-21 (δ_{H} 1.27)/C-17 (δ_{C} 158.9), and H-16 (δ_{H} 5.71)/C-13 (δ_{C} 46.9), while confirming the absence of a hydroxy group at C-14, suggested the presence of a 16,17-ene moiety in **3** (Figures S15 and S59, Supporting Information). The ECD spectrum of **3** showed a positive Cotton effect at 342 nm, which confirmed the stereochemistry of the ring A/B linkage as being the same as that in **1**.²¹ On the basis of the foregoing evidence, the structure of perulactone K was determined as (24*S*,25*R*)-5 β ,6 β -epoxy-20 β ,22 α ,28-trihydroxy-1-oxo-ergosta-2,16-dien-26-oic acid γ -lactone (**3**).

The HREIMS and ¹H and ¹³C NMR data of perulactone L (**4**) were consistent with the molecular formula C₂₈H₄₀O₇ and indicated that it is an isomer of perulactone B (**24**). The ¹H and ¹³C NMR spectra of **4** (Tables 1 and 3), assigned with the help of HSQC data (Supporting Information, Figures S19), were almost identical with those of perulactone B (**24**) except for the absence of signals due to the 2(3)-en-1-one moiety in ring A of **24**. Instead, the ¹H NMR spectrum of **4** exhibited signals due to a tetrasubstituted 3(4),5(6)-conjugated diene moiety [δ 6.02 (1H, dd, J = 9.6 and 2.8 Hz), 5.61 (1H, ddd, J = 9.6, 4.4, and 2.8 Hz), and 5.66 (1H, t, J = 4.0 Hz)]. These data suggested that **4** is isomeric with **24** and that they differ from each other by virtue of the position of the olefinic double bond in ring A. Finally, treatment of **24** with NaCN–MeOH resulted in the isomerization of its 1-oxo-2(3),5(6)-diene moiety to a 1-oxo-3(4),5(6)-diene unit, affording **4**. Thus, the structure of perulactone L was determined as (24*S*,25*R*)-14 α ,17 β ,20 β ,22 α ,28-pentahydroxy-1-oxo-ergosta-3,5-dien-26-oic acid γ -lactone (**4**).

Withanolide **5** was determined to have the molecular formula C₂₈H₃₈O₇, based on its HRESIMS and NMR data. The ¹H NMR spectrum of **5** (Table 2) showed signals due to H-3 [δ_{H} 6.83 (1H, ddd, J = 10.0, 6.4, 2.4 Hz)], H-2 [δ_{H} 6.00 (1H, dd, J = 10.0, 2.0 Hz)], H-6 [δ_{H} 3.18 (1H, d, J = 2.0 Hz)], H-22 [δ_{H} 4.04 (1H, d, J = 8.8 Hz)], five methyl groups, and an oxygenated methine group [δ_{H} 4.38 (1H, brd, J = 8.8 Hz)]. Comparison of the ¹³C NMR data of **5** (Table 3) with those of withanolide E (**13**)¹⁴ revealed that the CH₂-23 group in **13** is replaced by an oxygenated methine [δ_{C} 67.1], and the presence of a methine signal at δ_{C} 49.0 suggested that C-17 of **5** is not oxygenated. A long-range correlation observed for

H₃-28 and C-23 in its HMBC spectrum (Figure S25, Supporting Information) further supported the presence of OH-23 in **5**, whereas long-range correlations of H₃-18 (δ_{H} 1.01)/C-17 and H₃-21 (δ_{H} 1.33)/C-17 suggested the presence of a methine proton at C-17, confirming that **5** is a 17-deoxy-23-hydroxy analogue of withanolide E (**13**). The large coupling constant ($J = 8.8$ Hz) observed for H-22/H-23 of **5** was consistent with the relevant dihedral angle of 45° for the favorable conformation adopted by ring E with a β -OH at C-23 as in 23 β -hydroxyphysacoctolide.¹³ The β -orientation of its side chain at C-17 was deduced from the NOE correlation observed for H₃-18/H₃-21 (Figure S26, Supporting Information). The ECD spectrum of **5** exhibited positive Cotton effects at 265 and 339 nm, suggesting the 22*R* configuration²¹ and the *cis*-linkage of rings A/B.²¹ Thus, the structure of **5** was established as 17-deoxy-23 β -hydroxywithanolide E [(17*S*,20*S*,22*R*)-5 β ,6 β -epoxy-14 α ,20,23 β -trihydroxy-1-oxowitha-2,24-dienolide].

The HREIMS and NMR data of withanolide **6** were consistent with the molecular formula C₂₈H₃₈O₈. Its ¹H NMR spectrum (Table 2) exhibited signals due to H-3 [δ_{H} 6.79 (1H, ddd, $J = 10.0, 6.4, 2.4$ Hz)], H-2 [δ_{H} 6.00 (1H, dd, $J = 10.0, 2.4$ Hz)], H-6 [δ_{H} 3.17 (1H, brs)], H-22 [δ_{H} 4.76 (1H, d, $J = 10.8$ Hz)], five methyl groups, and an oxygenated methine group [δ_{H} 4.27 (1H, brd, $J = 10.8$ Hz)]. Comparison of the ¹³C NMR data of **6** (Table 3) with those of withanolide E (**13**)¹⁴ revealed that the CH₂-23 in **13** is replaced by an oxygenated methine (δ_{C} 66.4) in **6**. Therefore, **6** was suspected to be a 23-hydroxy analogue of withanolide E. In its HMBC spectrum, the presence of a correlation between H₃-28 and C-23 supported the presence of OH-23 in **6** (Figure S31, Supporting Information and Figure 2). The large coupling constant observed for H-22/H-23 ($J = 10.8$ Hz) of **6** similar to those of **5** and 23 β -hydroxyphysacoctolide¹³ suggested that the orientation of OH-23 is β . The ECD spectrum of **6** showed positive Cotton effects at 265 and 339 nm, suggesting a 22*R* configuration²¹ and *cis*-linkage of rings A/B.²¹ On the basis of the foregoing evidence, the structure of withanolide **6** was elucidated as 23 β -hydroxywithanolide E [(20*S*,22*R*)-5 β ,6 β -epoxy-14 α ,17 β ,20,23 β -tetrahydroxy-1-oxowitha-2,24-dienolide].

The molecular formula of withanolide **7** was determined to be C₂₈H₃₆O₆ using a combination of HRESIMS and ¹³C NMR data and accounted for 11 degrees of unsaturation. Comparison of its ¹H and ¹³C NMR data (Tables 2 and 3) with those of withanolide E (**13**) and phyperunolide A (**14**) indicated that **7** contains 2,3-en-1-one, 5 β ,6 β -epoxide, and side chain δ -lactone moieties similar to those in **13** and a 16,17-ene moiety as in **14**. The ¹H and ¹³C NMR data [δ_{H} 5.77 (1H, dd, $J = 3.6, 1.2$ Hz); δ_{C} 124.3 (CH) and 156.4 (C)] further suggested the presence of a 16,17-double bond in **7**, which was confirmed by the correlations of H₃-18 [δ_{H} 1.12 (3H, s)]/C-17 [δ_{C} 156.4 (C)] and H₃-21 [δ_{H} 1.27 (3H, s)]/C-17 observed in its HMBC spectrum (Figure S36, Supporting Information). The absolute configuration of C-22 was determined as *R* from the positive Cotton effect at 257 nm in its ECD spectrum.²¹ Thus, withanolide **7** was identified as 4-deoxyphyperunolide A [(20*S*,22*R*)-5 β ,6 β -epoxy-14 α ,20-dihydroxy-1-oxowitha-2,16,24-trienolide].

Withanolides **8** and **9** were determined to have the same molecular formula (C₂₈H₃₈O₇) by the analysis of their HREIMS and ¹³C NMR data, indicating that they are isomeric with each other and both are mono-oxygenated analogues of withanolide F (**22**),²⁰ a compound also encountered in the same plant extract. Comparison of the ¹H NMR and ¹³C NMR data

of **8** (Tables 2 and 3) with those of **22** suggested them to be very similar except that one of the carbocyclic ring CH₂ groups of **22** underwent hydroxylation, leading to a CH-OH [δ_{H} 4.28 (1H, d, $J = 8.8$ Hz); δ_{C} 65.9 (CH)] moiety present in **8**. The HMBC correlations of H-7 (δ_{H} 4.28)/C-5 (δ_{C} 136.3) and H₃-19 (δ_{H} 1.20)/C-5 observed for **8** (Figure S41, Supporting Information) suggested that this OH is attached to C-7, and the NOE correlation of H-7/H-9 α (δ_{H} 2.33) (Figure S42, Supporting Information) helped to determine the orientation of OH-7 as β . The strong positive Cotton effect at 252 nm in the ECD spectrum suggested a 22*R* configuration.²¹ The structure of withanolide **8** was thus established as 7 β -hydroxywithanolide F [(20*S*,22*R*)-7 β ,14 α ,17 β ,20-tetrahydroxy-1-oxowitha-2,5,24-trienolide (**8**)]. The ¹H NMR spectrum of withanolide **9** lacked resonances due to the ring A 2,3-en-1-one moiety, but exhibited signals due to a tetrasubstituted 3(4),5(6)-conjugated diene moiety [δ 6.01 (1H, dd, $J = 10.0$ and 2.4 Hz), 5.67 (1H, ddd, $J = 10.0$, 4.4, and 2.8 Hz), and 5.50 (1H, d, $J = 2.8$ Hz)], similar to that of perulactone L (**4**). In its ¹H NMR spectrum, **9** showed the presence of a CHOH group [δ_{H} 4.38 (1H, brd, $J = 6.4$)], as in **8**. The HMBC correlations of H-7 (δ_{H} 4.38)/C-5 (δ_{C} 141.6) and H₃-19 (δ_{H} 1.36)/C-5 (δ_{C} 141.6) for **9** (Figure S46, Supporting Information) suggested that this CHOH group is located at C-7, and the NOE correlation of H-7/H-9 α (δ_{H} 2.54) (Figure S47, Supporting Information) confirmed its orientation as β . The absolute configuration of C-22 was determined as *R* from the strong positive Cotton effect at 254 nm in its ECD spectrum²¹ (Figure S61, Supporting Information). Thus, the structure of withanolide **9** was elucidated as 7 β -hydroxy-17-*epi*-withanolide K [(20*S*,22*R*)-7 β ,14 α ,17 β ,20-tetrahydroxy-1-oxowitha-3,5,24-trienolide].

The HRESIMS and ¹³C NMR data of withanolide **10** were consistent with the molecular formula C₂₈H₄₀O₇. The ¹H and ¹³C NMR spectra of **10** (Tables 2 and 3), assigned with the help of the HSQC and HMBC data (Figures S51 and S52, Supporting Information), suggested that **10** contains ring A 2,3-en-1-one, ring B 5,6-ene, 14 α -OH, and 20-OH moieties similar to those of withanolide G,²⁰ but the structure of the side chain δ -lactone moiety differed from any of the known withanolides. The presence of only four methyl signals including one doublet and three singlets in its ¹H NMR spectrum suggested that ring E of **10** constituted a saturated δ -lactone and that one of the side chain methyl groups (CH₃-27 or CH₃-28) has undergone oxidation to a CH₂OH [δ_{H} 3.86 (1H, brd, $J = 11.0$ Hz), 3.65 (1H, dd, $J = 11.0$, 7.8 Hz)]. The ¹³C NMR spectrum of **10** (Table 3), assigned with the help of HSQC data, while confirming the presence of ring A 2,3-en-1-one [δ_{C} 204.2 (C-1), 145.3 (CH-3), 128.0 (CH-2)], ring B 5,6-ene [δ_{C} 135.1 (C-5), 125.0 (CH-6)], and four methyls [δ_{C} 20.8 (CH₃-21), 18.9 (CH₃-19), 17.7 (CH₃-18), 14.3 (CH₃-27)], suggested that it contains a saturated δ -lactone [δ_{C} 177.8 (C-26)], five oxygenated carbons [δ_{C} 84.4 (C-14), 81.4 (CH-23), 77.2 (C-20), 76.7 (CH-22), 63.2 (CH₂-28)], and a methine carbon (C-17) at 49.8 ppm. These assignments were supported by the long-range correlations of H₃-19/C-1, H₃-19/C-6, H-3/C-1, and H-4/C-6 for rings A/B; H₃-18/C-14, H₃-18/C-17, and H-17/C-21 for ring D; and H₃-27/C-26, H₃-27/C-24, H-23/C-25, H-23/C-28, and H-22/C-21 for ring E in the HMBC spectrum of **10** (Figure S52, Supporting Information). The orientation of the side chain at C-17 was determined to be β by the NOESY correlation between H₃-18 and H₃-21. Additional NOESY correlations observed for the ring E protons, H-23 α with H-22 α , H₂-28 α , and H-25 α of **10** (Figure S53, Supporting Information), suggested that OH-23, H-24, and CH₃-25 are β -oriented. The positive Cotton effect at 278 nm in the ECD spectrum

of **10** (Figure S61, Supporting Information) suggested a 22*R* configuration.²¹ Thus, withanolide **10** was identified as 24,25-dihydro-23 β ,28-dihydroxywithanolide G [(20*S*, 22*R*)-14 α ,20,23 β ,28-tetrahydroxy-1-oxowitha-2,5-dienolide].

The molecular formula of withanolide **11** (C₂₈H₄₀O₇) and its ¹H and ¹³C NMR data (Tables 2 and 3) indicated that it is an analogue of withanolide E (**13**) in which the double bond of ring E has undergone reduction. The ¹³C NMR data for **11** suggested the presence of a carbonyl of a saturated δ -lactone ring (δ_C 175.4), and its ¹H NMR spectrum showed doublets for CH₃-27 [δ_H 1.21 (3H, d, *J* = 6.8 Hz)] and CH₃-28 [δ_H 1.12 (3H, d, *J* = 6.8 Hz)]. These assignments for CH₃-27 and CH₃-28 were confirmed by the long-range correlations of H₃-27/C-26, H₂-23/C-25, and H₂-23/C-28 observed in its HMBC spectrum (Figure S57, Supporting Information). The relative configuration of these methyl groups was established by NOESY correlations of H₃-28/H-25 [δ_H 2.16 (1H, m)], H₃-28/H-22, and H-22/H-25 (Figure S58, Supporting Information), suggesting that the saturated δ -lactone of ring E of **11** possesses the same twist boat conformation, with equatorial orientations of CH₃-27 and CH₃-28, as in philadelphicalactone A.²³ The absolute configuration of C-22 was determined as *R* from the positive Cotton effect at 278 nm in its ECD spectrum (Figure S61, Supporting Information).²¹ On the basis of the foregoing evidence, the structure of withanolide **11** was established as 24, 25 - dihydrowithanolide E [(20*S*,22*R*,24*S*,25*R*)-5 β ,6 β -epoxy-14 α ,17 β ,20-trihydroxy-1-oxowitha-2-enolide].

Withanolides **1–25** were evaluated for their cytotoxic activity in a panel of selected tumor cell lines consisting of LNCaP (androgen-sensitive human prostate adenocarcinoma), 22Rv1 (androgen-resistant human prostate adenocarcinoma), ACHN (human renal adenocarcinoma), M14 (human melanoma), SK-MEL-28 (human melanoma), and normal HFF (human foreskin fibroblast) cells. Physachenolide C (**26**), which we have previously shown to exhibit selective and potent activity for LNCaP cells,^{15,22} was used for comparison purposes. Of the withanolides tested, only 17 β -hydroxywithanolides (17-BHWs), **6, 8, 9, 11–13, 15, 19–22**, and **26**, exhibited cytotoxicity to LNCaP cells at a concentration below 2.0 μ M. The IC₅₀ data for the active withanolides are presented in Table 4. Interestingly, the order of activity of these 17-BHWs (**13** > **20** > **22** > **12** > **21** > **11** > **8** > **15** > **19** > **9**) was found to be almost the same for both PC cell lines, LNCaP and 22Rv1, except for **6**, with a β -OH group at C-23, which was active against 22Rv1 cells with an IC₅₀ of 0.89 \pm 0.1 μ M, but had no activity for LNCaP cells at 2.0 μ M. The cytotoxicity data for LNCaP cells for these 17-BHWs suggested that a ring A 2,3-en-1-one and α -oriented unsaturated δ -lactone side chain and/or a β -OH at C-17 are essential for their activity and acetoxylation at C-18 leads to 3-fold enhancement of activity (**26** vs **13**). These data also provided additional structure–activity relationship (SAR) information for 17-BHWs, including decreases in activity due to (i) isomerization of the 2,3-ene to 3,4-ene (**8** vs **9**); (ii) β -hydroxylation at C-4 (**12** vs **13**); (iii) β -methoxylation at C-4 (**15** vs **13**); (iv) replacement of the 5 β ,6 β -epoxide with 5,6-ene (**22** vs **13**); (v) β -hydroxylation at C-7 (**19** vs **13** and **8** vs **22**); (vi) reduction of the 24,25-double bond of the side chain (**11** vs **13**); and (vii) hydroxylation at C-28 (**21** vs **22**). Intriguingly, of the 26 withanolides tested, only three (**13**, **20**, and **26**) showed selectivity for renal carcinoma (ACHN) cells (Table 4). Although there appears to be no direct correlation between cytotoxic activities for ACHN and LNCaP cells, it is noteworthy

that withanolides **13**, **20**, and **26**, found to be active against ACHN cells, are those with the highest potency for LNCaP cells. Nonetheless, the prostate cancer cell lines were still much more sensitive to the effects of active 17-BHWs. In addition to supporting our previous findings that α -orientation of the side chain and/or the presence of a β -OH at C-17 of withanolides may have a significant influence on their selectivity to certain cancer cell lines, these SAR data for 17-BHWs suggest the importance of the structure of the side chain for their activity and potency.

EXPERIMENTAL SECTION

General Experimental Procedures.

Optical rotations were measured with a JASCO Dip-370 polarimeter using MeOH as the solvent. UV spectra were recorded with a Shimadzu UV 2601 spectrophotometer. ECD spectra were measured with a JASCO J-810 spectropolarimeter. 1D and 2D NMR spectra were recorded in CDCl₃ using residual solvent as the internal standard on a Bruker Avance III 400 spectrometer at 400 MHz for ¹H NMR and 100 MHz for ¹³C NMR, respectively. The chemical shift values (δ) are given in parts per million (ppm), and the coupling constants (J values) are in Hz. Low-resolution MS were recorded on a Shimadzu LCMS-QP8000 α and high-resolution MS on a Agilent G6224A TOF mass spectrometer. Analytical thin-layer chromatography (TLC) was carried out on silica gel 60 F₂₅₄ aluminum-backed TLC plates (Merck), and preparative TLC was performed on Analtech silica gel 500 μ m glass plates. Compounds were visualized with short-wave UV and by spraying with anisaldehyde-sulfuric acid reagent and heating until the spots appeared. Silica gel flash chromatography was accomplished using 230–400 mesh silica gel. Sephadex LH-20 for gel-permeation chromatography was obtained from Amersham Biosciences. HPLC purifications were carried out using a 10 \times 250 mm Phenomenex Luna 5 μ m C₁₈ (2) column for reversed-phase (RP) chromatography and a 10 \times 250 mm Econosil Si (10 μ) column for normal-phase (NP) chromatography, with a Waters Delta Prep system consisting of a PDA 996 detector. When required, MM2 energy minimizations of all possible conformers were carried out using Chem3D 15.0 from PerkinElmer, Inc.

Aerobic Cultivation and Harvesting of *P. peruviana*.

The seeds of *P. peruviana* obtained from Trade Wind Fruit (P.O. Box 1102, Windsor, CA, USA) were germinated in 1.0 in. Grodan rock-wool cubes in a Barnstead Lab-line growth chamber kept at 28 °C with 16 h of fluorescent lighting and maintaining 25–50% humidity. After ca. 4 weeks in the growth chamber, seedlings with an aerial length of ca. 5.0 cm were transplanted to aeroponic culture boxes for further growth, as described previously for *Withania somnifera* and *Physalis crssifolia*.^{13,24} A herbarium sample was deposited at the University of Arizona Natural Products Center (accession number NPC-DB-11/5/10). Aerial parts of aeroponically grown plants were harvested when fruits were almost mature (ca. 2 months under aeroponic growth conditions). Harvested plant materials were dried in the shade, powdered, and stored at 5 °C prior to extraction.

Extraction and Isolation of Withanolides.

Dried and powdered aerial parts of aeroponically grown *P. peruviana* (1.2 kg) were divided into four portions, and each portion was extracted with 60% aqueous MeOH (3.0 L) in an ultrasonic bath at 25 °C for 2 h and then allowed to stand for 8 h. After filtration, the resulting filtrates were combined and passed through a column packed with HP-20SS resin (2.0 kg). The column was first eluted with 60% MeOH(aq) (4.0 L) followed by MeOH (5.0 L). The crude withanolide extract (24.5 g) obtained by concentrating the MeOH eluates was subjected to column chromatography on RP C₁₈ (400.0 g) and eluted with 2.0 L each of 50%, 60%, and 70% MeOH(aq) and MeOH to afford five fractions, A–E: A (3.5 g) eluted with 50% MeOH(aq); B (4.2 g) with 60% MeOH(aq); C (3.1 g) with 60–70% MeOH(aq); D (4.3 g) with 70% MeOH(aq); and E (8.2 g) with MeOH. Of these, fractions B–D, which contained withanolides, were further purified as described below. Fraction B (4.2 g) on purification by column chromatography over silica gel (200 g) and elution with EtOAc gave 4 β -hydroxywithanolide E (**12**) (1.6 g) and an impure fraction (242 mg). This impure fraction was purified by RP HPLC [60% MeOH(aq)] followed by silica gel preparative TLC [CHCl₃–MeOH (95:5)] to afford **1** (6.2 mg, *R_f* 0.4) and additional 4 β -hydroxywithanolide E (**12**) (181 mg). A portion of fraction C (2.0 g) was further fractionated by silica gel (250 g) column chromatography and elution with EtOAc (1.0 L), EtOAc–MeOH (98:2) (1.0 L), and MeOH (500 mL), affording seven subfractions, C₁–C₇: C₁ (125.0 mg) eluted with EtOAc; C₂ (610.0 mg) with EtOAc; C₃ (95.0 mg) with EtOAc; C₄ (285.0 mg) with EtOAc; C₅ (195.0 mg) with EtOAc–MeOH (98:2); C₆ (67 mg) with EtOAc–MeOH (98:2); and C₇ (550.0 mg) with MeOH. A portion of subfraction C₂ (400.0 mg) was subjected to further fractionation by silica gel (20 g) column chromatography and elution with CHCl₃–MeOH (99:1) (200 mL), CHCl₃–MeOH (98:2) (200 mL), and CHCl₃–MeOH (95:5) (200 mL). The resulting fractions were combined based on their TLC profiles to afford nine subfractions (C₂₋₁–C₂₋₉). On further purification by RP HPLC, subfraction C₂₋₂ (8.5 mg) afforded **14** [4.0 mg, *t_R* 25.0 min, 55% MeOH(aq)]; subfraction C₂₋₄ (37.0 mg) gave **22** [1.4 mg, *t_R* 33.0 min, 65% MeOH(aq)], **25** [2.0 mg, *t_R* 22.0 min, 65% MeOH(aq)], and **13** [16.0 mg, *t_R* 17.0 min, 65% MeOH(aq)]; subfraction C₂₋₅ (26.0 mg) afforded **3** [8.8 mg, *t_R* 24.0 min, 60% MeOH(aq)] and **23** [2.1 mg, *t_R* 14.0 min, 60% MeOH(aq)]. Subfraction C₂₋₆ (95.0 mg) was fractionated by column chromatography on silica gel (20.0 g), and elution with EtOAc provided three subfractions, C₂₋₆₋₁ (40.0 mg), C₂₋₆₋₂ (17.0 mg), and C₂₋₆₋₃ (17.0 mg). Further purification of subfraction C₂₋₆₋₁ (40 mg) by RP HPLC afforded **17** [3.3 mg, *t_R* 11.0 min, 65% MeOH(aq)] and **24** [20.0 mg, *t_R* 18.0 min, 65% MeOH(aq)]. When purified by RP HPLC, subfraction C₂₋₆₋₁ gave **5** [1.2 mg, *t_R* 24.0 min, 55% MeOH(aq)], **6** [3.3 mg, *t_R* 32.0 min, 55% MeOH(aq)], and **3** [1.5 mg, *t_R* 36.0 min, 55% MeOH(aq)]. Fraction C₂₋₇ (170.0 mg) was subjected to column chromatography on silica gel (20.0 g) and eluted with CHCl₃–MeOH (95:5) to afford a withanolide-containing fraction (152.0 mg). Further purification of this fraction (20.0 mg) by silica gel preparative TLC (EtOAc) gave **20** (11.6 mg, *R_f* 0.4) and **21** (1.8 mg, *R_f* 0.5). Subfraction C₂₋₈ (24.0 mg) was subjected to column chromatography on silica gel (8 g), and elution with EtOAc afforded **8** (15.0 mg) and a fraction (5.2 mg) that was further purified by RP HPLC [60% MeOH(aq)] to give **9** (2.7 mg, *t_R* 29.0 min). A portion of subfraction C₄ (150.0 mg) was purified by column chromatography over silica gel (8 g) and elution with CH₂Cl₂–MeOH (95:5) to obtain a

fraction (52.6 mg), which, on further purification by RP HPLC using 60% MeOH(aq), afforded **19** (27.0 mg, t_R 20.0 min) and **8** (11.0 mg, t_R 25.0 min). Purification of subfraction C₅ by column chromatography over silica gel (8 g) and elution with CH₂Cl₂–MeOH (9:1) afforded **18** (35.0 mg). Fraction D (4.0 g) was separated by column chromatography over silica gel (250 g), and elution with EtOAc afforded withanolide E (**13**, subfraction D₂, 2.2 g) and two subfractions, D₁ (245.0 mg) and D₃ (108.0 mg). A portion (100.0 mg) of subfraction D₁ was fractionated by RP HPLC using 65% MeOH(aq) to yield three subfractions, D₁₋₁ (35.8 mg, t_R 18.0 min), D₁₋₂ (6.2 mg, t_R 22.0 min), and D₁₋₃ (4.7 mg, t_R 25.0 min). Subfraction D₁₋₁ was further purified by column chromatography on silica gel (8 g), and elution with CHCl₃–MeOH (95:5) afforded **3** (1.5 mg), **7** (3.3 mg), and **24** (20 mg). Purification of subfractions D₁₋₂ by preparative TLC [silica gel; CHCl₃–MeOH (95:5)] gave **2** (4.8 mg), and purification of D₁₋₃ by the same procedure afforded **4** (2.1 mg) and **25** (2.0 mg). Further purification of subfraction D₃ by RP HPLC using 65% MeOH(aq) yielded three subfractions: D₃₋₁ (50.1 mg), D₃₋₂ (25.2 mg), and D₃₋₃ (24.4 mg), and subsequent purification of these subfractions by column chromatography over silica gel with CHCl₃–MeOH (99:1 and 98:2) gave **16** (10.5 mg) and **18** (6.1 mg) from subfraction D₃₋₁, **10** (3.5 mg) and **11** (1.5 mg) from subfraction D₃₋₂, and **15** (1.4 mg) and **25** (10.2 mg) from subfraction D₃₋₃.

Perulactone I (1): amorphous, colorless powder; $[\alpha]_D^{25} + 85$ (c 0.24, MeOH); UV (MeOH) λ_{max} (log ϵ) 223 (3.81) nm; ECD (MeOH) $[\theta]$ –4345 (242 nm), +3766 (340 nm); ¹H and ¹³C NMR data, see Tables 1 and 3, respectively; positive HRESIMS m/z 527.2620 [M + Na]⁺ (calcd for C₂₈H₄₀O₈Na, 527.2621).

Perulactone J (2): amorphous, colorless powder; $[\alpha]_D^{25} + 9$ (c 0.09, MeOH); UV (MeOH) λ_{max} (log ϵ) 224 (3.76) nm; ECD (MeOH) $[\theta]$ +7461 (254 nm), –7491 (339 nm); ¹H and ¹³C NMR data, see Tables 1 and 3, respectively; positive HRESIMS m/z 495.2720 [M + Na]⁺ (calcd for C₂₈H₄₀O₆Na, 495.2723).

Perulactone K (3): amorphous, colorless powder; $[\alpha]_D^{25} + 49$ (c 0.11, MeOH); UV (MeOH) λ_{max} (log ϵ) 222 (3.89) nm; ECD (MeOH) $[\theta]$ –2170 (242 nm), +1331 (264 nm), +2031 (342 nm); ¹H and ¹³C NMR data, see Tables 1 and 3, respectively; positive HRESIMS m/z 493.2554 [M + Na]⁺ (calcd for C₂₈H₃₈O₆Na, 493.2566).

Perulactone L (4): amorphous, colorless powder; $[\alpha]_D^{25} + 52$ (c 0.20, MeOH); UV (MeOH) λ_{max} (log ϵ) 230 (3.84) nm; ECD (MeOH) $[\theta]$ +10 095 (245 nm), –1400 (310 nm), –710 (342 nm, sh.); ¹H and ¹³C NMR data, see Tables 1 and 3, respectively; positive HRESIMS m/z 511.2670 [M + Na]⁺ (calcd for C₂₈H₄₀O₇Na, 511.2672).

17-Deoxy-23β-hydroxywithanolide E (5): amorphous, colorless powder; $[\alpha]_D^{25} - 3.0$ (c 0.12, MeOH); UV (MeOH) λ_{max} (log ϵ) 223 (4.02) nm; ECD (MeOH) $[\theta]$ –13 854 (231 nm), +440 (266 nm), +1858 (339 nm); ¹H and ¹³C NMR data, see Tables 1 and 3,

respectively; positive HRESIMS m/z 509.2502 $[M + Na]^+$ (calcd for $C_{28}H_{38}O_7Na$, 509.2515).

23 β -Hydroxywithanolide E (6): amorphous, colorless powder; $[\alpha]_D^{25} + 37$ (c 0.30, MeOH); UV (MeOH) λ_{max} ($\log \epsilon$) 221 (3.97) nm; ECD (MeOH) $[\theta]$ -8240 (239 nm), +187 (264 nm), +2728 (339 nm); 1H and ^{13}C NMR data, see Tables 2 and 3, respectively; positive HRESIMS m/z 525.2449 $[M + Na]^+$ (calcd for $C_{28}H_{38}O_8Na$, 525.2464).

4-Deoxyhyperunolide A (7): amorphous, colorless powder; $[\alpha]_D^{25} + 65$ (c 0.16, MeOH); UV (MeOH) λ_{max} ($\log \epsilon$) 228 (4.06) nm; ECD (MeOH) $[\theta]$ +11 244 (257 nm), +6149 (341 nm); 1H and ^{13}C NMR data, see Tables 2 and 3, respectively; positive HRESIMS m/z 491.2408 $[M + Na]^+$ (calcd for $C_{28}H_{36}O_6Na$, 491.2410).

7 β -Hydroxywithanolide F (8): amorphous, colorless powder; $[\alpha]_D^{25} + 124$ (c 0.49, MeOH); UV (MeOH) λ_{max} ($\log \epsilon$) 225 (4.12) nm; ECD (MeOH) $[\theta]$ +27 006 (252 nm), -7184 (338 nm); 1H and ^{13}C NMR data, see Tables 2 and 3, respectively; positive HRESIMS m/z 509.2496 $[M + Na]^+$ (calcd for $C_{28}H_{38}O_7Na$, 509.2515).

7 β -Hydroxy-17-epi-withanolide K (9): amorphous, colorless powder; $[\alpha]_D^{25} + 131$ (c 0.26, MeOH); UV (MeOH) λ_{max} ($\log \epsilon$) 224 (4.15) nm; ECD (MeOH) $[\theta]$ +22 189 (254 nm), -2517 (307 nm); 1H and ^{13}C NMR data, see Tables 2 and 3, respectively; positive HRESIMS m/z 509.2509 $[M + Na]^+$ (calcd for $C_{28}H_{38}O_7Na$, 509.2515).

24,25-Dihydro-23 β ,28-dihydroxywithanolide G (10): amorphous, colorless powder; $[\alpha]_D^{25} + 4$ (c 0.16, MeOH); UV (MeOH) λ_{max} ($\log \epsilon$) 223 (3.65) nm; ECD (MeOH) $[\theta]$ +5674 (254 nm), -8022 (307 nm); 1H and ^{13}C NMR data, see Tables 2 and 3, respectively; positive HRESIMS m/z 511.2667 $[M + Na]^+$ (calcd for $C_{28}H_{40}O_7Na$, 511.2672).

24,25-Dihydrowithanolide E (11): amorphous, colorless powder; $[\alpha]_D^{25} + 48$ (c 0.15, MeOH); UV (MeOH) λ_{max} ($\log \epsilon$) 224 (3.76) nm; ECD (MeOH) $[\theta]$ -2660 (242 nm), +1541 (278 nm), +3916 (339 nm); 1H and ^{13}C NMR data, see Tables 2 and 3, respectively; positive HRESIMS m/z 511.2660 $[M + Na]^+$ (calcd for $C_{28}H_{40}O_7Na$, 511.2672).

Epoxidation of Perulactone B (24).—To a stirred solution of **24** (2.0 mg) in CH_2Cl_2 (1.0 mL) was added *m*-chloroperbenzoic acid (2.0 mg), and the mixture was stirred at 25 °C. After 3 h (TLC control), the reaction mixture was partitioned between $CHCl_3$ (5.0 mL) and water (10.0 mL). The $CHCl_3$ layer was washed with water (10.0 mL), dried (Na_2SO_4), and subjected to purification by silica gel preparative TLC [$CHCl_3$ -MeOH (95:5)] to afford the major β -epoxidation product as an off-white, amorphous powder (1.0 mg). The 1H and ^{13}C NMR and APCIMS data of this product were identical with those of **1** obtained above.

Conversion of Perulactone B (24) to Perulactone L (4).—To a stirred solution of **24** (2.0 mg) in MeOH (1.0 mL) was added NaCN (1.0 mg), and the mixture was stirred at 25 °C. After 2 h (TLC control), the reaction mixture was concentrated using a flow of N₂, and the residue thus obtained was dissolved in CHCl₃ (2.0 mL). The CHCl₃ solution was concentrated and was separated by silica gel preparative TLC [CHCl₃–MeOH (95:5)] to afford the product as an off-white, amorphous powder (1.9 mg). The APCIMS and ¹H and ¹³C NMR data of this product were identical with those of **4** obtained above.

Cytotoxicity Assay.

The ACHN, M14, and SK-MEL-28 cells were all obtained from the Developmental Therapeutics Program (NCI, Frederick, MD, USA). LNCaP and HFF cells were purchased from ATCC (Manassas, VA, USA), and the 22Rv1 cells were kindly provided by Dr. Len Neckers (NCI, Bethesda, MD, USA). Cell lines were maintained as recommended by the source institution. Cell numbers were estimated using the MTS dye assay (Promega, Madison, WI, USA).²⁵ The MTS dye assay was used for evaluating cytotoxicity of withanolides **1–26** against androgen-sensitive human prostate adenocarcinoma (LNCaP), androgen-resistant human prostate adenocarcinoma (22Rv1), human renal adenocarcinoma (ACHN), human melanoma (M14 and SK-MEL-28) cell lines, and human foreskin fibroblast cells. Doxorubicin and DMSO were used as positive and negative controls, respectively. For LNCaP, ACHN, 22Rv1, and HFF cells, the assay was performed in RPMI with 5% fetal calf serum, 2.0 mM L-glutamine, 1× nonessential amino acids, 1.0 mM sodium pyruvate, 100 U/mL penicillin, 100 µg/mL streptomycin, 10 mM HEPES, and 5 × 10⁻⁵ M 2-mercaptoethanol. For M14 and SK-MEL-28 cells, DMEM replaced RPMI. Briefly, 10 000 cells (LNCaP) or 5000 cells (22Rv1, ACHN, M14, SK-MEL-28, HFF) were incubated overnight at 37 °C in 96-well microtiter plates. Serial dilutions of compounds in DMSO or vehicle control (DMSO) were added to triplicate wells, and the microtiter plates were incubated for a further 72 h. Viable cell number was determined by the addition of CellTiter 96 Aqueous One Solution cell proliferation assay solution (MTS), plates were incubated for 2 h, and then absorbance (A) at 490 nm was measured. Cytotoxicity was calculated as in the following formula: % cytotoxicity = [(A_{Medium} - A_{Treatment})/A_{Medium}] × 100. The IC₅₀ values and standard deviations (±) were determined using Microsoft Excel software from dose–response curves obtained from at least three independent experiments.

Supplementary Material

Refer to Web version on PubMed Central for supplementary material.

ACKNOWLEDGMENTS

Financial support for this work from the College of Agriculture and Life Sciences and the School of Natural Resources and the Environment of the University of Arizona is gratefully acknowledged. This project has also been funded in whole or in part with federal funds from the National Cancer Institute, National Institutes of Health, under contract HHSN26120080001E. The content of this publication does not necessarily reflect the views or policies of the Department of Health and Human Services, nor does the mention of trade names, commercial products, or organizations imply endorsement by the U.S. Government. This research was supported [in part] by the Intramural Research Program of NIH, Frederick National Lab, Center for Cancer Research. We thank Mr. D. Bunting for his help with germination and aeroponic cultivation of *P. peruviana* used in this work.

REFERENCES

- (1). Schrijvers D; Van Erps P; Cortvriend J *Adv. Ther* 2010, 27, 285–296. [PubMed: 20532721]
- (2). Jemal A; Bray F; Center MM; Ferlay J; Ward E; Forman D *Ca-Cancer J. Clin* 2011, 61, 69–90. [PubMed: 21296855]
- (3). Phillips C *NCI Cancer Bull.* 2012, 9, 2.
- (4). Asangani IA; Dommeti VL; Wang X; Malik R; Cieslik M; Yang R; Escara-Wilke J; Wilder-Romans K; Dhanireddy S; Engelke C; Iyer MK; Jing X; Wu Y-M; Cao X; Qin ZS; Wang S; Feng FY; Chinnaiyan AM *Nature* 2014, 510, 278–282. [PubMed: 24759320]
- (5). Sanford M *Drugs* 2013, 73, 1723–1732. [PubMed: 24127223]
- (6). (a)Zegarra-Moro OL; Schmidt LJ; Huang H; Tindall DJ *Cancer Res.* 2002, 62, 1008–1013. [PubMed: 11861374] (b)Chen CD; Welsbie DS; Tran C; Baek SH; Chen R; Vessella R; Rosenfeld MG; Sawyers CL *Nat. Med* 2004, 10, 33–39. [PubMed: 14702632] (c)Attard G; Richards J; de Bono JS *Clin. Cancer Res* 2011, 17, 1649–1657. [PubMed: 21372223] (d)Tan MHE; Li J; Xu HE; Melcher K; Yong E *Acta Pharmacol. Sin* 2015, 36, 3–23. [PubMed: 24909511]
- (7). Key Statistics about Kidney Cancer. American Cancer Society Home Page. <http://www.cancer.org/cancer/kidneycancer/detailedguide/kidney-cancer-adult-key-statistics>.
- (8). (a)McDermott DI; Atkins MB *I Semin. Oncol* 2006, 33, 583–587. [PubMed: 17045087] (b)Cohen RB; Oudard S *Invest. New Drugs* 2012, 30, 2066–2079. [PubMed: 22327313]
- (9). Zhang W-N; Tong W-Y *Chem. Biodiversity* 2016, 13, 48–65.
- (10). Chen LX; He H; Qiu F *Nat. Prod. Rep* 2011, 28, 705–740. [PubMed: 21344104]
- (11). (a)Baumann TW; Meier CM *Phytochemistry* 1993, 33, 317–321.(b)Dinan LN; Sarker SD;Šik V *Phytochemistry* 1997, 44, 509–512.(c)Ahmad S; Malik A; Muhammad P; Gul W; Yasmin R; Afza N *Fitoterapia* 1998, 69, 433–436.(d)Ahmad S; Yasmin R; Malik A *Chem. Pharm. Bull* 1999, 47, 477–480.(e)Fang S-T; Li B; Liu J-K *Helv. Chim. Acta* 2009, 92, 1304–1308.(f)Lan Y-H; Chang F-R; Pan M-J; Wu C-C; Wu S-J; Chen S-L; Wang S-S; Wu M-J; Wu Y-C *Food Chem.* 2009, 116, 462–469.(g)Fang S-T; Liu J-K; Bo LJ *Asian Nat. Prod. Res* 2010, 12, 618–622.(h)Yen C-Y; Chiu C-C; Chang F-R; Chen JY-F; Hwang C-C; Hseu Y-C; Yang H-L; Lee AY-L; Tsai M-T; Guo Z-L; Cheng Y-S; Liu Y-C; Lan Y-H; Chang Y-C; Ko Y-C; Chang H-W; Wu Y-C *BMC Cancer* 2010, 10, 46. [PubMed: 20167063] (i)Fang S-T; Liu J-K; Li B *Steroids* 2012, 77, 36–44. [PubMed: 22037277] (j)Wang H-C; Tsai Y-L; Wu Y-C; Chang F-R; Liu M-H; Chen W-Y; Wu C-C *PLoS One* 2012, 7, e37764. [PubMed: 22701533] (k)Chiu C-C; Huang J-W; Chang F-R; Huang K-J; Huang H-M; Huang H-W; Chou C-K; Wu Y-C; Chang H-W *PLoS One* 2013, 8, e64739. [PubMed: 23705007] (l)You B-J; Wu Y-C; Lee C-L; Lee H-Z *Food Chem. Toxicol* 2014, 65, 205–212. [PubMed: 24373828] (m)Sang-Ngern M; Youn UJ; Park E-J; Kondratyuk TP; Simmons CJ; Wall MM; Ruf M; Lorch SE; Leong E; Pezzuto JM; Chang LC *Bioorg. Med. Chem. Lett* 2016, 26, 2755–2759. [PubMed: 27210437] (n)Park E-J; Sang-Ngern M; Chang LC; Pezzuto JM *Mol. Nutr. Food Res* 2016, 60, 1482–1500. [PubMed: 27006100]
- (12). Henrich CJ; Brooks AD; Erickson KL; Thomas CL; Bokesch HR; Tewary P; Thompson CR; Pompei RJ; Gustafson KR; McMahon JB; Sayers TJ *Cell Death Dis.* 2015, 6, e1666. [PubMed: 25719250]
- (13). Xu YM; Bunting DP; Liu MX; Bandaranayake HA; Gunatilaka AA L. *J. Nat. Prod* 2016, 79, 821–830. [PubMed: 27071003]
- (14). (a)Sahai M; Gottlieb HE; Ray AB; Ali A; Glotter E; Kirson IJ *Chem. Res. (S)* 1982, 346–347. (b)Gottlieb HE; Kirson I; Glotter E; Ray AB; Sahai M; Ali AJ *Chem. Soc., Perkin Trans I* 1986, 229–231.(c)Ozawa M; Morita M; Hirai G; Tamura S; Kawai M; Tsuchiya A; Oonuma K; Maruoka K; Sodeoka M *ACS Med. Chem. Lett* 2013, 4, 730–735. [PubMed: 24900739]
- (15). Damu AG; Kuo P-C; Su C-R; Kuo T-H; Chen T-H; Bastow KF; Lee K-H; Wu T-SJ *Nat. Prod* 2007, 70, 1146–1152.
- (16). Zviely M; Goldman A; Kirson I; Glotter EJ *Chem. Soc., Perkin Trans 1* 1986, 229–231.
- (17). Frolow F; Ray AB; Sahai M; Glotter E; Gottlieb HE; Kirson IJ *Chem. Soc., Perkin Trans 1* 1981, 1029–1032.

- (18). (a) Glotter E; Abraham A; Günzberg G; Kirson IJ *Chem. Soc., Perkin Trans 1* 1977, 341–346.
(b) Vitali G; Conte L; Nicoletti M *Planta Med.* 1996, 62, 287–288. [PubMed: 17252448]
- (19). Shingu K; Miyagawa M; Yahara S; Nohara T *Chem. Pharm. Bull* 1993, 41, 1873–1875.
- (20). Velde VV; Lavie D; Budhiraja RD; Sudhir S; Garg KN *Phytochemistry* 1983, 22, 2253–2257.
- (21). Moiseeva GP; Vasina OE; Abubakirov NK *Khim. Prir. Soedin* 1990, 3, 371–376.
- (22). Xu YM; Liu MX; Grunow N; Wijeratne EMK; Paine-Murrieta G; Felder S; Kris RM; Gunatilaka AA L. *J. Med. Chem* 2015, 58, 6984–6993. [PubMed: 26305181]
- (23). Su B-N; Misico R; Park EJ; Santarsiero BD; Mesecar AD; Fong HHS; Pezzuto JM; Kinghorn AD *Tetrahedron* 2002, 58, 3453–3466.
- (24). Xu YM; Gao S; Bunting DP; Gunatilaka AA L. *Phytochemistry* 2011, 72, 518–522. [PubMed: 21315384]
- (25). Brooks AD; Jacobsen KM; Li W; Shankar A; Sayers TJ *Mol. Cancer Res* 2010, 8, 729–738. [PubMed: 20442297]

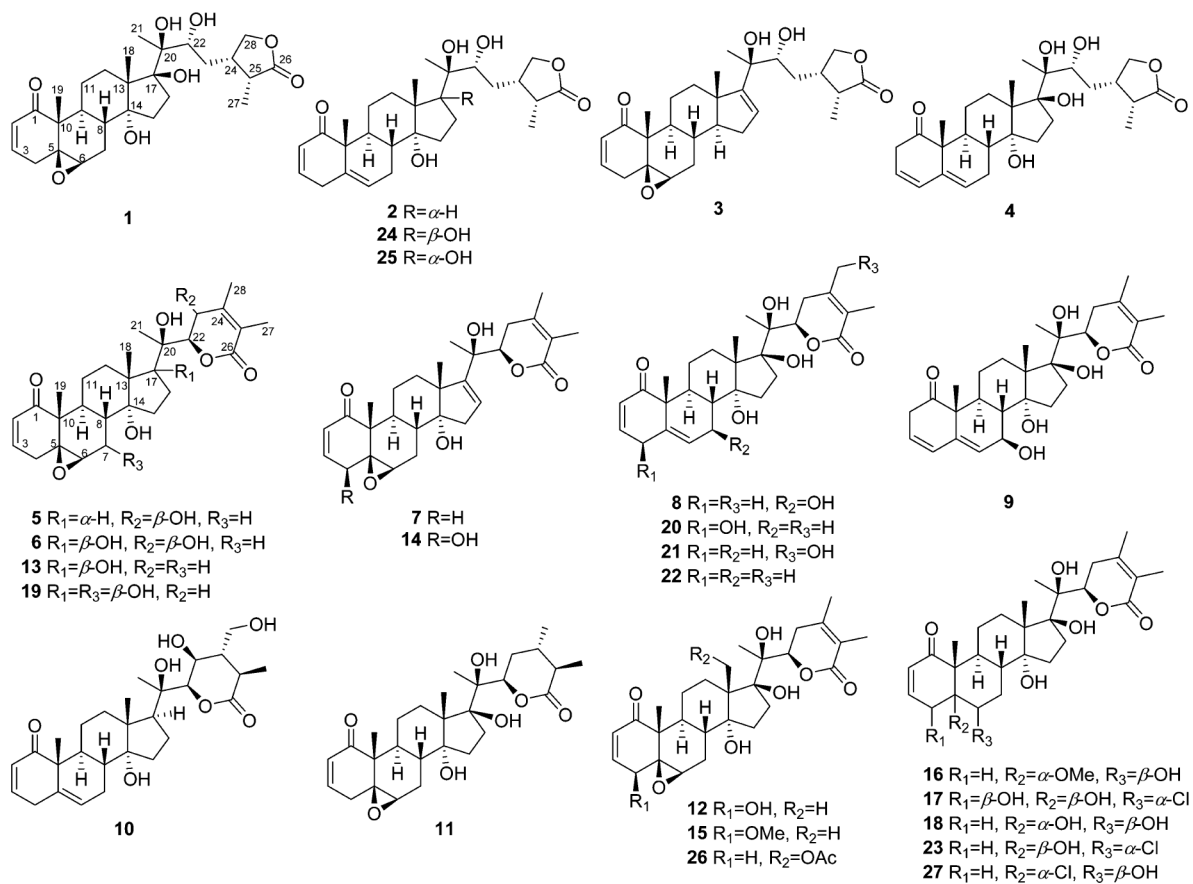


Figure 1. Structures of withanolides 1–25 from aeroponically grown *P. peruviana*, physachenolide C (26), and withanolide C (27).

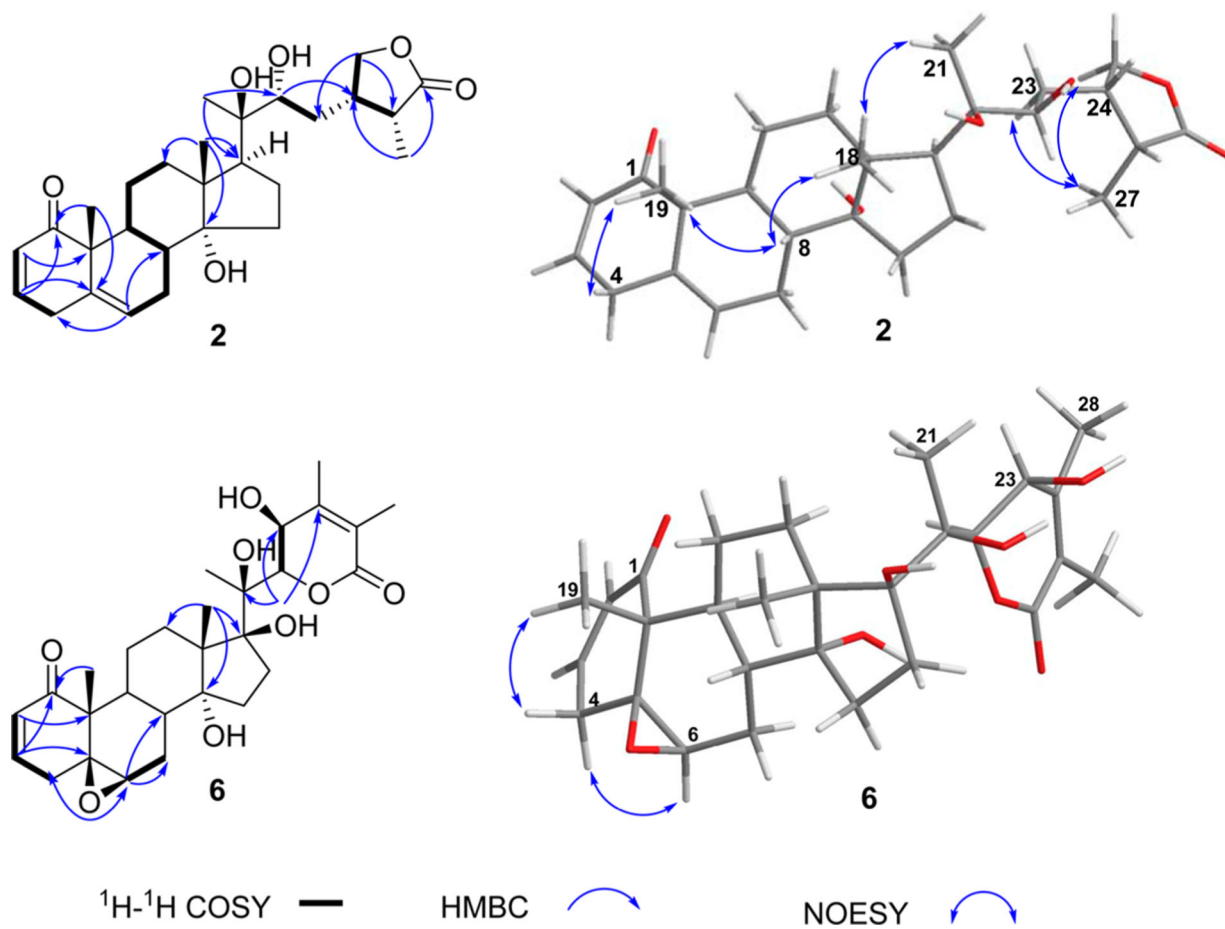


Figure 2.
Key HMBC, ^1H - ^1H COSY, and NOE correlations of withanolides 2 and 6.

Table 1.

¹H NMR Data (400 MHz, δ , Hz) for Perulactones I–L (1–4) in CDCl₃^a

position	1	2	3	4
2	5.99 dd (10.0, 2.8)	5.87 dd (10.0, 2.0)	6.01 dd (10.0, 2.4)	2.72 dd (20.0, 4.4) 3.29 brd (20.0)
3	6.85, ddd (10.0, 6.4, 2.0)	6.77 ddd (10.0, 4.8, 2.4)	6.84 ddd (10.0, 6.4, 2.4)	5.61 ddd (9.6, 4.4, 2.8)
4	1.92 m	2.83 dd (21.2, 4.8)	1.90 m	6.02 dd (9.6, 2.8)
6	2.96 brd (19.2)	3.27 brd (21.2)	2.98 dt (18.8, 2.8)	5.66 t (4.0)
7	3.19 d (2.0)	5.59 brd (5.6)	3.14 d (2.8)	2.09 m
	1.97 m	2.03 m	2.08 m	2.03 m
	1.80 m	1.82 m	1.34 m	1.99 m
8	1.86 m	1.84 m	1.78 m	2.36 m
9	2.33 m	2.00 m	1.19 m	1.93 m
11	2.08 m	2.20 m	2.13 m	1.48 m
	1.62 m	1.54 m	1.54 m	1.73 m
12	2.20 m	1.80 m	1.97 m	1.56 m
	1.47 m	1.55 m	1.49 m	
14			1.32 m	
15	1.67 m	1.79 m	2.10 m	2.08 m
	1.52 m	1.52 m	1.89 m	1.27 m
16	2.62 m	1.66 m	5.71 dd (2.4, 1.2)	2.67 m
	1.43 m	1.85 m		1.44 m
17		2.25 m		
18	1.08 s	1.03 s	0.94 s	1.12 s
19	1.26 s	1.23 s	1.25 s	1.38 s
21	1.22 s	1.20 s	1.27 s	1.23 s
22	4.01 brd (10.4)	3.46 dd (10.8, 1.6)	3.65 dt (10.4, 2.0)	4.11 brd (10.4)
23	2.12 m	1.63 m	1.70 m	2.38 m
	1.33 m	1.24 m	1.47 m	1.67 m
24	2.71 q (7.2)	2.70 m	2.60–2.75 m	2.53 m
25	2.65 m	2.65 m	2.60–2.75 m	2.52 m

position	1	2	3	4
27	1.16 d (7.2)	1.16 d (7.6)	1.16 d (7.2)	1.13 d (7.6)
28	4.06 dd (8.8, 8.4)	4.10 dd (9.2, 8.4)	4.14 dd (9.2, 7.6)	4.03 dd (8.8, 7.6)
	4.39 dd (8.8, 7.2)	4.43 dd (9.2, 7.2)	4.43 dd (9.2, 6.8)	4.31 dd (8.8, 6.8)

^a Assignments based on DEPT, HSQC, and HMBC data.

Table 2.

¹H NMR Data (400 MHz, δ, Hz) for Withanolides 5–11 in CDCl₃^a

position	5	6	7	8	9	10	11
2	6.00 dd (10.0, 2.0)	6.00 dd (10.0, 2.4)	6.01 dd (10.0, 2.8)	5.81, dd (10.0, 2.0)	2.70 dd (20.2, 4.8) 3.24 dt (20.0, 2.4)	5.86 ddd (10.0, 3.0, 1.0)	6.01 dd (10.0, 3.0)
3	6.83 ddd (10.0, 6.4, 2.4)	6.79 ddd (10.0, 6.4, 2.4)	6.80 ddd (10.0, 6.4, 2.0)	6.73 ddd (10, 4.8, 2.4)	5.67 ddd (10.0, 4.4, 2.8)	6.76 ddd (10.0, 5.0, 2.5)	6.80 ddd (10.0, 6.5, 2.2)
4	1.90 m	1.84 m	1.83 dd (18.4, 6.4)	2.81 dd (21.2, 4.8)	6.01 dd (10.0, 2.4)	2.82 dd (21.2, 5.0)	1.84 dd (18.4, 6.5)
6	2.96 dt (18.8, 2.8)	2.92 dt (18.4, 2.8)	2.92 ddd (18.4, 2.8, 2.0)	3.24 dt (21.2, 2.4)		3.27 brd (21.2)	2.93 dt (18.4, 2.6)
7	3.18 d (2.0)	3.17 brs	3.17 brs	5.43 brs	5.50 d (2.8)	5.59 brd (5.5)	3.17 brs
8	1.92 m	1.95 m	2.08 m	4.28 d (8.8)	4.38 brd (6.4)	2.08 m	1.94 m
9	1.82 m	1.91 m	1.93 m			1.81 m	
10	1.95 m	1.91 m	1.98 m	1.67 dd (12.0, 8.8)	1.79 m	1.82 m	1.89 m
11	1.61 m	1.88 m	1.88 m	2.33 m	2.54 m	2.09 m	1.88 m
12	1.98 m	2.03 m	2.02 m	2.28 m	1.91 m	2.18 m	2.06 m
15	1.52 m	1.57 m	1.56 m	1.56 m	1.37 m	1.56 m	1.63 m
16	1.67–1.75 m	2.19 dt (4.0, 12.0)	2.12 m	2.38 m	2.41 m	1.97 m	2.33 m
17	1.67 m	1.67 m	1.43, m	1.26 m	1.24 m	1.72 m	1.39 m
18	1.57 m	1.67 m	2.19 dd (14.4, 3.6)	1.89 m	1.93 m	1.52 m	1.63 m
19	1.48 m	1.60 m	2.31 dd (14.4, 1.2)	1.78 m	1.75 m	1.82 m	1.54 m
20	2.05 m	2.77 ddd (14.8, 11.6, 8.8)	5.77 dd (3.6, 1.2)	2.62 m	2.66 m	1.82 m	2.68 m
21	1.83 m	1.53 m		1.41 m	1.43 m	1.40 m	1.40 m
22	2.50 t (9.2)					2.64 t (9.4)	
23	1.01 s	1.07 s	1.12 s	1.05 s	1.07 s	1.01 s	1.09 s
24	1.24 s	1.21 s	1.23 s	1.20 s	1.36 s	1.23 s	1.24 s
25	1.33 s	1.45 s	1.27 s	1.35 s	1.36 s	1.33 s	1.35 s
26	4.04 d (8.8)	4.76 d (10.8)	4.39 dd (12.8, 3.6)	4.88 dd (12.4, 4.4)	4.87 dd (12.0, 4.8)	3.55 d (7.4)	4.89 dd (11.0, 3.4)
27	4.38 brd (8.8)	4.27 brd (10.8)	2.78 brt (15.2) 2.14 m	2.40–2.55 m	2.40–2.55 m	4.18 t (7.4)	1.92 m
28							1.82 m
29							1.70 m
30							2.16 m
31	1.88 s	1.89 s	1.85 brs	1.82 s	1.82 s	1.28 d (6.8)	1.21 d (6.8)

Author Manuscript

Author Manuscript

Author Manuscript

Author Manuscript

3.65 dd (11.0, 7.8) 3.86 brd (11.0) 1.12 d (6.8) 1.89 s 1.89 s 1.95 s 1.97 s 1.95 s 28

^pAssignments based on DEPT, HSQC, and HMBC data.

Table 3.

^{13}C NMR Data (100 MHz) of Withanolides 1–11 in CDCl_3^a

position	1	2	3	4	5	6	7	8	9	10	11
1	203.8 C	204.1 C	203.3 C	211.0 C	203.5 C	202.9 C	202.8 C	203.7 C	209.9 C	204.2 C	203.0 C
2	129.2 CH	127.9 CH	129.3 CH	39.8 CH ₂	129.4 CH	129.8 CH	130.0 CH	127.9 CH	39.6 CH ₂	128.0 CH	129.9 CH
3	144.7 CH	145.3 CH	144.3 CH	126.8 CH	144.3 CH	143.6 CH	143.5 CH	144.9 CH	123.9 CH	145.3 CH	143.7 CH
4	33.0 CH ₂	33.4 CH ₂	33.0 CH ₂	129.2 CH	33.0 CH ₂	32.9 CH ₂	32.8 CH ₂	32.8 CH ₂	128.6 CH	33.5 CH ₂	32.8 CH ₂
5	62.1 C	135.2 C	62.1 C	141.0 C	61.9 C	62.2 C	62.2 C	136.3 C	141.6 C	135.1 C	62.1 C
6	64.0 CH	124.8 CH	63.2 CH	121.9 CH	64.0 CH	64.1 CH	63.8 CH	129.8 CH	130.7 CH	125.0 CH	64.1 CH
7	26.3 CH ₂	25.3 CH ₂	30.9 CH ₂	25.8 CH ₂	26.2 CH ₂	26.3 CH ₂	26.0 CH ₂	65.9 CH	66.3 CH	25.3 CH ₂	26.2 CH ₂
8	34.0 CH	35.1 CH	28.5 CH	35.6 CH	32.3 CH	34.1 CH	31.2 CH	45.1 CH	44.4 CH	35.3 CH	34.1 CH
9	36.9 CH	36.3 CH	44.9 CH	34.1 CH	37.4 CH	36.7 CH	37.0 CH	34.4 CH	33.3 CH	36.2 CH	36.8 CH
10	48.5 C	50.8 C	48.5 C	52.4 C	48.5 C	48.6 C	48.6 C	50.2 C	52.0 C	50.7 C	48.6 C
11	23.2 CH ₂	22.1 CH ₂	23.4 CH ₂	21.7 CH ₂	22.4 CH ₂	22.7 CH ₂	21.8 CH ₂	22.8 CH ₂	21.6 CH ₂	22.2 CH ₂	22.9 CH ₂
12	30.0 CH ₂	32.5 CH ₂	36.0 CH ₂	32.3 CH ₂	32.1 CH ₂	30.1 CH ₂	28.4 CH ₂	30.2 CH ₂	30.0 CH ₂	32.3 CH ₂	30.4 CH ₂
13	54.2 C	47.4 C	46.9 C	54.6 C	47.6 C	54.8 C	52.3 C	54.8 C	54.9 C	47.3 C	54.7 C
14	83.2 C	84.6 C	58.1 CH	83.7 C	84.9 C	82.1 C	84.5 C	81.7 C	81.4 C	84.4 C	81.9 C
15	32.5 CH ₂	32.0 CH ₂	30.9 CH ₂	31.6 CH ₂	32.5 CH ₂	32.3 CH ₂	39.9 CH ₂	34.9 CH ₂	34.6 CH ₂	32.2 CH ₂	32.4 CH ₂
16	37.6 CH ₂	20.9 CH ₂	126.9 CH	37.7 CH ₂	21.3 CH ₂	37.8 CH ₂	124.3 CH	37.6 CH ₂	37.7 CH ₂	20.8 CH ₂	37.8 CH ₂
17	88.3 C	49.4 CH	158.9 C	88.3 C	49.0 CH	88.1 C	156.4 C	86.7 C	86.9 C	49.8 CH	87.7 C
18	20.6 CH ₃	17.4 CH ₃	17.9 CH ₃	20.6 CH ₃	17.5 CH ₃	20.4 CH ₃	20.6 CH ₃	20.5 CH ₃	20.5 CH ₃	17.7 CH ₃	20.6 CH ₃
19	15.2 CH ₃	18.9 CH ₃	14.9 CH ₃	20.2 CH ₃	15.2 CH ₃	14.6 CH ₃	14.2 CH ₃	18.5 CH ₃	19.9 CH ₃	18.9 C	14.5 CH ₃
20	78.5 C	77.5 CH	76.7 C	79.0 C	77.1 C	79.5 C	74.7 C	78.6 C	78.6 C	77.2 C	79.2 C
21	19.3 CH ₃	20.2 CH ₃	23.1 CH ₃	19.0 CH ₃	24.1 CH ₃	19.3 CH ₃	22.41 CH ₃	19.1 CH ₃	19.2 CH ₃	20.8 CH ₃	17.2 CH ₃
22	72.3 CH	75.2 CH	74.6 CH	72.6 CH	85.6 CH	82.4 CH	79.4 CH	80.7 CH	80.5 CH	76.7 CH	78.9 CH
23	31.9 CH ₂	28.8 CH ₂	27.3 CH ₂	29.9 CH ₂	67.1 CH	66.4 CH	29.8 CH ₂	34.3 CH ₂	34.3 CH ₂	81.4 CH	33.2 CH ₂
24	38.1 CH	38.1 CH	37.9 CH	38.1 CH	151.7 C	153.4 C	149.3 C	151.3 C	151.2 C	37.2 CH	31.8 CH
25	37.7 CH	37.7 CH	37.9 CH	37.8 CH	121.9 C	121.1 C	127.6 C	121.1 C	121.2 C	49.6 CH	40.7 CH
26	180.8 C	180.4 C	180.3 C	180.8 C	164.1 C	164.2 C	165.2 C	167.2 C	167.0 C	177.8 C	175.4 C
27	10.5 CH ₃	10.5 CH ₃	10.5 CH ₃	10.6 CH ₃	12.9 CH ₃	12.8 CH ₃	12.4 CH ₃	12.1 CH ₃	12.2 CH ₃	14.3 CH ₃	14.4 CH ₃

position	1	2	3	4	5	6	7	8	9	10	11
28	72.5 CH ₂	72.2 CH ₂	72.4 CH ₂	73.0 CH ₂	15.7 CH ₃	15.5 CH ₃	22.4 CH ₃	20.6 CH ₃	20.6 CH ₃	63.2 CH ₂	21.4 CH ₃

^a Assignments based on DEPT, HSQC, and HMBC data.

^b Assignments are interchangeable.

Cytotoxicity Data of Withanolides from Aeronically Cultivated *Physalis peruviana* against a Panel of Selected Tumor Cell Lines and Normal Cells^a

Table 4.

compound	cell line ^b							
	LNCaP	22Rv1	ACHN	M14	SK-MEL-28	HFF		
6	>2	0.89 ± 0.10	>2	>2	>2	>2		
8	0.33 ± 0.04	0.56 ± 0.01	>2	>2	>2	>2		
9	0.94 ± 0.10	0.99 ± 0.08	>2	>2	>2	>2		
11	0.29 ± 0.05	0.21 ± 0.02	>2	>2	>2	>2		
12	0.16 ± 0.04	0.09 ± 0.01	>2	>2	>2	>2		
13	0.06 ± 0.01	0.07 ± 0.01	0.46 ± 0.06	>2	>2	>2		
15	0.33 ± 0.02	0.24 ± 0.03	>2	>2	>2	>2		
19	0.33 ± 0.02	0.26 ± 0.02	>2	>2	>2	>2		
20	0.11 ± 0.01	0.07 ± 0.01	1.0 ± 0.08	>2	>2	>2		
21	0.24 ± 0.02	0.21 ± 0.02	>2	>2	>2	>2		
22	0.13 ± 0.10	0.07 ± 0.02	>2	>2	>2	>2		
26	0.02 ± 0.01	0.03 ± 0.01	0.57 ± 0.06	>2	>2	>2		
doxorubicin	0.02 ± 0.01	0.02 ± 0.01	0.02 ± 0.01	0.09 ± 0.01	0.25 ± 0.01	0.15 ± 0.03		

^aResults are expressed as IC₅₀ values in μ M. Doxorubicin and DMSO were used as positive and negative controls. Withanolides **1-5**, **7**, **10**, **14**, **16-18**, and **23-25** had no activity up to 5.0 μ M.

^bKey: LNCaP = androgen-sensitive human prostate adenocarcinoma; 22Rv1 = androgen-resistant human prostate adenocarcinoma; ACHN = human renal adenocarcinoma; M14 = human melanoma; SK-MEL-28 = human melanoma; HFF = human foreskin fibroblast.